



OPEN

Levosimendan increases brain tissue oxygen levels after cardiopulmonary resuscitation independent of cardiac function and cerebral perfusion

Andreas García-Bardon¹✉, Jens Kamuf¹, Alexander Ziebart¹, Tanghua Liu¹, Nadia Krebs¹, Bastian Dünge¹, Robert F. Kelm¹, Svenja Morsbach², Kristin Mohr², Axel Heimann³, Erik K. Hartmann¹ & Serge C. Thal^{1,4}✉

Prompt reperfusion is important to rescue ischemic tissue; however, the process itself presents a key pathomechanism that contributes to a poor outcome following cardiac arrest. Experimental data have suggested the use of levosimendan to limit ischemia–reperfusion injury by improving cerebral microcirculation. However, recent studies have questioned this effect. The present study aimed to investigate the influence on hemodynamic parameters, cerebral perfusion and oxygenation following cardiac arrest by ventricular fibrillation in juvenile male pigs. Following the return of spontaneous circulation (ROSC), animals were randomly assigned to levosimendan (12 µg/kg, followed by 0.3 µg/kg/min) or vehicle treatment for 6 h. Levosimendan-treated animals showed significantly higher brain PbtO₂ levels. This effect was not accompanied by changes in cardiac output, preload and afterload, arterial blood pressure, or cerebral microcirculation indicating a local effect. Cerebral oxygenation is key to minimizing damage, and thus, current concepts are aimed at improving impaired cardiac output or cerebral perfusion. In the present study, we showed that NIRS does not reliably detect low PbtO₂ levels and that levosimendan increases brain oxygen content. Thus, levosimendan may present a promising therapeutic approach to rescue brain tissue at risk following cardiac arrest or ischemic events such as stroke or traumatic brain injury.

Abbreviations

BL	Baseline
CA	Cardiac arrest
CBF	Cerebral blood flow
CI	Cardiac index
CPR	Cardiopulmonary resuscitation
GEDI	Global end-diastolic volume index
ITBI	Intrathoracic blood volume index
LEVO	Levosimendan
MAP	Mean arterial blood pressure
NIRS	Near-infrared spectroscopy
PbtO ₂	Brain tissue oxygen

¹Department of Anesthesiology, Medical Center, Johannes Gutenberg-University, Langenbeckstraße 1, 55131 Mainz, Germany. ²Max Planck Institute for Polymer Research, Ackermannweg 10, 55128 Mainz, Germany. ³Institute for Neurosurgical Pathophysiology, Medical Center, Johannes Gutenberg-University, Mainz, Germany. ⁴Department of Anesthesiology, HELIOS University Hospital Wuppertal, Witten/Herdecke University, Heusnerstraße 40, 42283 Wuppertal, Germany. ✉email: a.garciabardon@uni-mainz.de; serge@thal.de

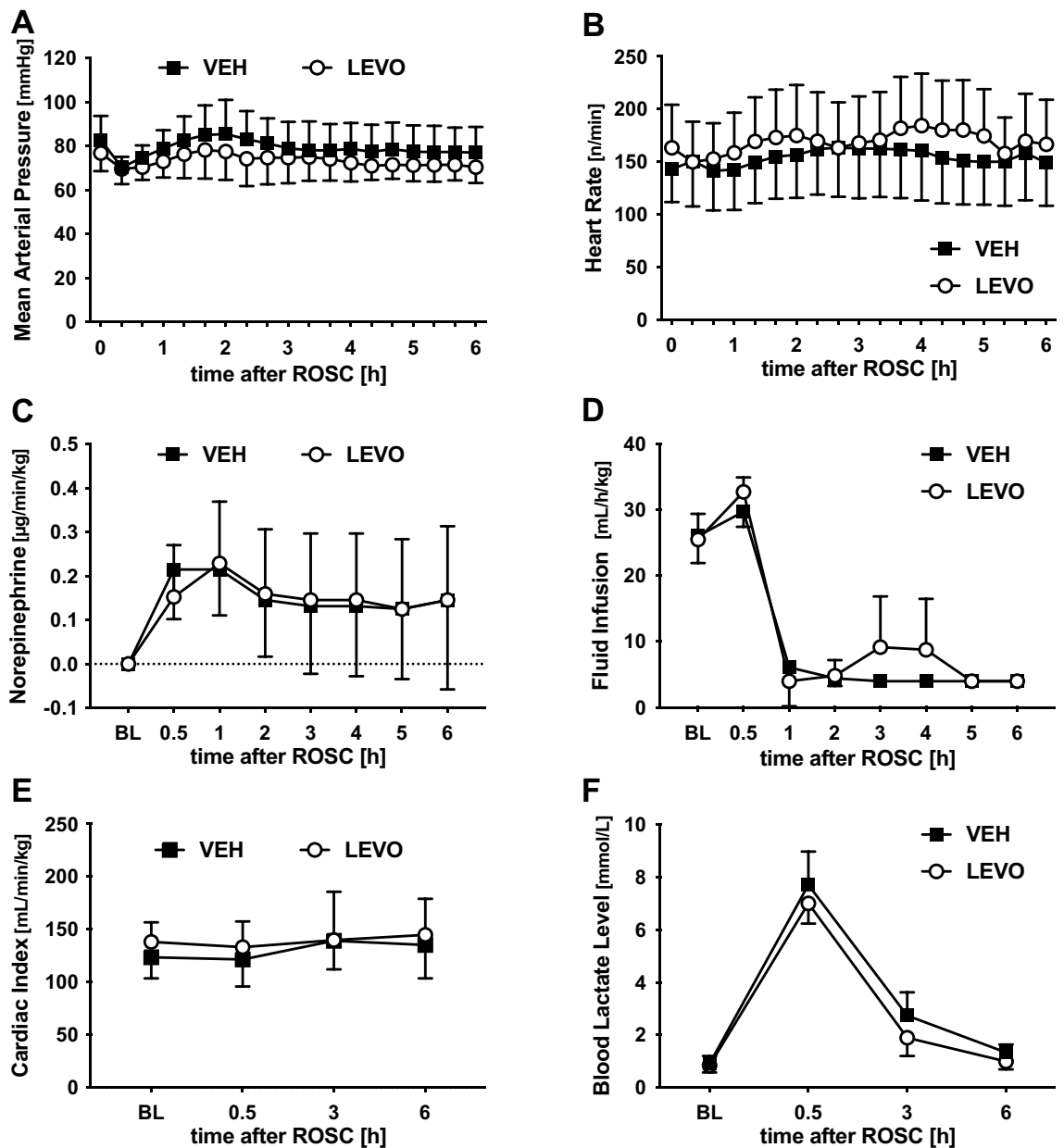


Figure 1. Cardiac index (CI), mean arterial pressure (MAP), and key experimental parameters. To determine the influence of cardiac arrest and levosimendan on key cardiovascular parameters and post-CPR management, MAP (A) and heart rate (B) were recorded before and after ROSC. MAP was maintained with (C) norepinephrine and (D) balanced electrolyte solution infusion. (E) As a general marker for cardiac function, CI was determined before and 0.5, 3, and 6 h after ROSC using the PiCCO System. (F) As a general marker for tissue hypoxia, blood lactate was quantified at the same time points. Levosimendan did not influence any parameter compared with vehicle treatment. *BL* baseline, *VEH* vehicle, *LEVO* levosimendan. Statistics: repeated measures two-way ANOVA, followed by Šidák's multiple comparisons test; data are presented as means \pm SD.

ROSC Return of spontaneous circulation
 rSO₂ Cerebral oxygen hemoglobin saturation
 SVRI Systemic vascular resistance index
 VEH Vehicle solution
 VF Ventricular fibrillation

Despite the increased number of successful resuscitations following cardiac arrest (CA) over the last decade, survival and discharge rates as well as long-term outcomes have not improved substantially¹. Hence, this discrepancy between successful resuscitation and patient outcome requires more effective and novel therapeutic strategies to achieve good neurocognitive function, which is the ultimate goal.

Levosimendan is an inodilator and calcium (Ca^{2+}) sensitizer that was clinically established for the treatment of acute heart failure². Because of its combination of inotropic and vasoactive characteristics, levosimendan has become a promising agent for post-CA care. Potential benefits during cardiopulmonary resuscitation (CPR) have been addressed in several studies, which have reported increased rates of return of spontaneous circulation (ROSC)³ and reduced rates of neuronal injury⁴ and organ ischemia/reperfusion injury⁵. These effects have been attributed to the known mechanisms of action of Ca^{2+} sensitization and activation of ATP-sensitive K^+ channels in the vascular bed and activation of mitochondrial ATP-sensitive K^+ channels in cardiomyocytes⁶. These regulations result in positive inotropy and peripheral and coronary vasodilation.

In isolated hippocampal mouse brain slices subjected to mechanical trauma, levosimendan was shown to reduce tissue injury⁷. Moreover, after 40 min of aortic clamping and consecutive spinal cord ischemia, levosimendan-treated rabbits showed better neurologic outcomes⁸. These results indicate a neuroprotective effect of levosimendan that cannot be attributed to cardiovascular changes but instead suggests a direct cellular effect on damaged tissue.

The causal link between myocardial stimulation and the observed protection following CA has not yet been determined. This study aimed to examine the significance of the cardiovascular system for levosimendan-mediated protection in a porcine model of CA by targeting the effects of levosimendan on global cerebral perfusion, cerebral microcirculation, and systemic hemodynamic parameters and correlating these changes with brain tissue oxygen levels and cerebral oxygen saturation.

Results

Experimental setting. ROSC was achieved in 16 of 19 animals, and all animals with ROSC survived the observation period. Before CPR, the experimental groups did not differ in terms of MAP, arterial and central venous oxygenation, lactate, total norepinephrine dose, or total amount of fluid infusion. The total length of ischemia and time from VF induction to ROSC were similar across both groups (LEVO: 674 ± 24 s, VEH: 668 ± 18 s). In all 16 animals, ROSC was achieved after a total dose of 0.8 U/kg vasopressin and a second defibrillation (360 J).

Blood pressure and heart rate. MAP and heart rate were recorded throughout the experiments and did not differ between the two groups (Fig. 1A,B). Similarly, vasopressor dose and balanced electrolyte solution volume required to maintain target MAP did not significantly differ between the two groups (fluid balance: LEVO: 33 mL/kg, VEH: 30 mL/kg; norepinephrine dose: LEVO: 0.15 $\mu\text{g}/\text{kg}/\text{min}$, VEH: 0.22 $\mu\text{g}/\text{kg}/\text{min}$) (Fig. 1C,D).

Cardiac index. To determine the influence of levosimendan on post-CPR myocardial dysfunction, CI was quantified using the thermo-dilution technique and normalized to body weight. As expected, in animals without preexisting cardiovascular pathology, CI was only temporarily impaired immediately after ROSC and recovered within 30 min to prearrest baseline values (LEVO: 138 mL/min/kg; VEH: 124 mL/min/kg; Fig. 1E). Moreover, there was no significant difference between the two groups.

Influence on serum lactate. As a marker of global tissue ischemia, serum lactate increased from normal baseline values noticeably, 30 min after ROSC (LEVO: 0.9–7.7 mmol/L; VEH: 0.85–7.0 mmol/L; Fig. 1F). In the further course, lactate returned to baseline levels within 6 h and did not differ significantly between the two groups.

Global parameters of cardiac preload and afterload. GEDI (Fig. 2A) and ITBI (Fig. 2B) describe changes in volume status at the end of the diastole and the estimated blood volume in the thorax, respectively, and were used as parameters for cardiac preload. SVRI was used as a parameter for cardiac afterload (Fig. 2C) to describe the influence of levosimendan on vascular resistance. None of the three parameters were significantly influenced by treatment.

Cerebral perfusion. To determine changes in cerebral perfusion, we used two independent techniques before and 30 min, 3 h, and 6 h after ROSC: global cerebral blood flow (CBF) was measured on the basis of fluorescent microspheres (Fig. 3A), and brain cortical blood flow was determined via O₂C (Fig. 3B). To compare cerebral perfusion with perfusion in other organ systems, at all time points, total blood flow in the kidney was defined as the index (Fig. 3C). To correct for interindividual variation, all parameters were normalized to the individual baseline level obtained before CA. Total cerebral perfusion (Fig. 3A) was stable during the experiments and was not influenced by levosimendan. In contrast to total cerebral perfusion data, regional cortical blood flow (Fig. 3B) decreased significantly to 72% of baseline for VEH and 63% of baseline for LEVO following ROSC and returned to baseline values at 3 and 6 h after ROSC. In contrast to cortical cerebral perfusion, and similarly to total brain perfusion, kidney perfusion did not differ between LEVO and VEH treatment groups (Fig. 3C).

Cerebral oxygenation. To identify changes in cerebral oxygenation, we used two independent techniques. We measured cortical rSO₂ using NIRS (Fig. 4A) and PbtO₂ in the frontal cortex using real-time O₂ fluorescence quenching (Fig. 4B). To avoid injury to the dura mater before CA and CPR, and to prevent mechanical brain tissue injury during the CPR procedure, we did not attempt to place the brain tissue probes before CPR, and the placement of the Foxy probe was performed immediately after ROSC. To maintain optimal blood oxygenation, ventilation was adjusted as described above. Settings were confirmed by arterial blood gas analysis. Using these

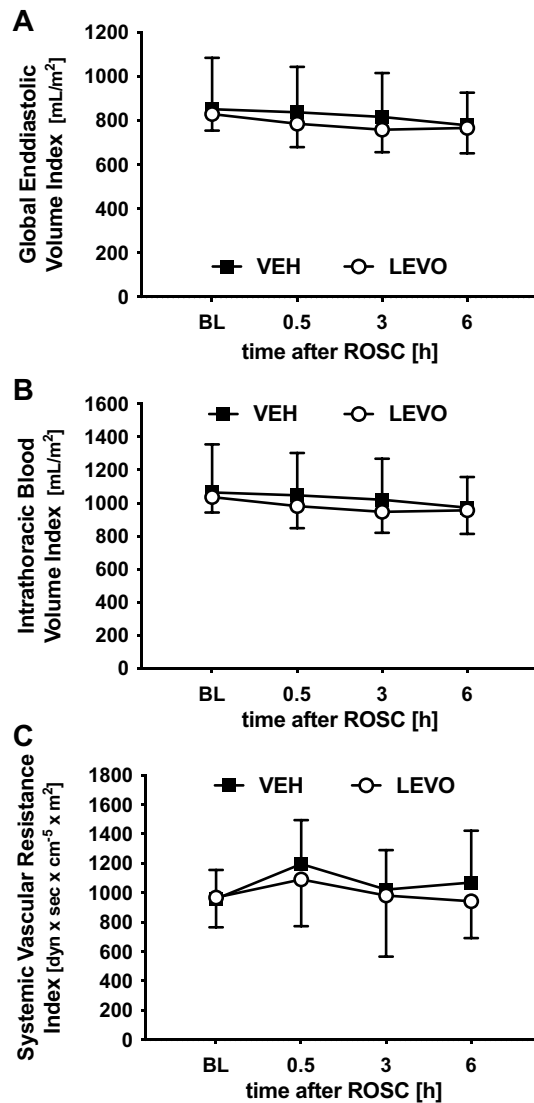


Figure 2. Surrogate parameters for cardiac preload and afterload. (A) Global end-diastolic volume index (GEDI) and (B) intrathoracic blood volume index as surrogate parameters for cardiac preload were determined using the PiCCO System before and 0.5, 3, and 6 h after ROSC to investigate changes in diastolic volume filling and diastolic function after cardiac arrest (CA) and levosimendan treatment. (C) To determine the influence on cardiac afterload, systemic vascular resistance index (SVRI) was recorded. CA and levosimendan did not influence any parameter at the selected time points. BL baseline, VEH vehicle, LEVO levosimendan. Statistics: repeated measures two-way ANOVA, followed by Šidák's multiple comparisons test; data are presented as means \pm SD.

settings, German landrace pigs typically show a PbtO₂ of 39.8 mmHg as recently demonstrated by our research team⁹.

NIRS values were normalized to the individual baseline level obtained prior to CA. rSO₂ was not altered by treatment with levosimendan (Fig. 4A). In contrast to the NIRS readings, PbtO₂ was significantly lower 30 min after ROSC. Changes in PbtO₂ were in line with changes in cortical perfusion 30 min after ROSC. Although cortical perfusion was not improved by levosimendan, PbtO₂ was significantly higher in the LEVO group at 30 min (LEVO: 66.0 \pm 24.1 mmHg vs. VEH: 34.1 \pm 17.4 mmHg, $p=0.0227$) and 3 h (LEVO: 53.9 \pm 14.3 mmHg vs. VEH: 29.9 \pm 13.2 mmHg, $p=0.0151$) after ROSC (Fig. 4B). This levosimendan-mediated increase of PbtO₂ was independent of CI (Fig. 4C) in the levosimendan-treated animals, which all showed normal PbtO₂, whereas PbtO₂ correlated with CI in the vehicle-treated animals ($r=0.6464$, $p=0.011$). Although mean PbtO₂ was in the normal range (25–50 mmHg) for both treatment groups, some of the vehicle-treated animals showed pathologically low PbtO₂ (Fig. 4C).

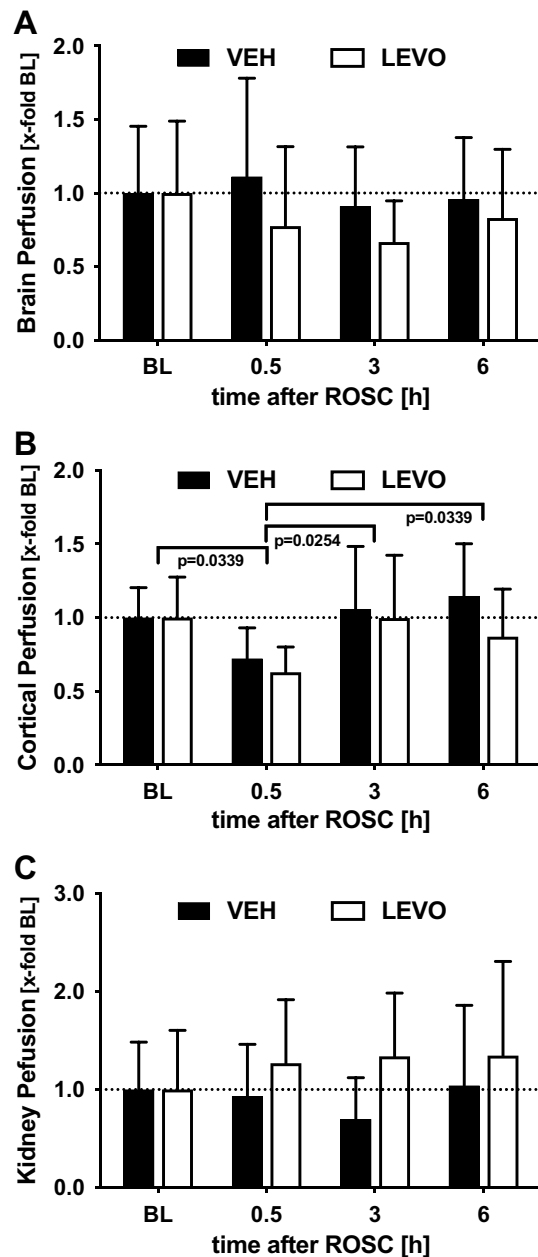


Figure 3. Cerebral and kidney perfusion. (A) Global cerebral blood flow was determined before and 0.5, 3, and 6 h after ROSC using fluorescent microspheres, and values were normalized to baseline values to correct for interindividual variation. (B) Cortical blood flow was measured with an epidural laser Doppler probe. (C) To show systemic perfusion, the kidney was selected as the index organ, and renal blood flow was measured using fluorescent microspheres. Although global brain and renal perfusion were not influenced by cardiac arrest (CA) or levosimendan treatment, brain cortical perfusion was significantly impaired 30 min after CA and returned to baseline levels at later time points. *BL* baseline, *VEH* vehicle, *LEVO* levosimendan. Statistics: repeated measures two-way ANOVA, followed by Šidák's multiple comparisons test; data are presented as means \pm SD.

Discussion

This is the first report to directly show that levosimendan improves cerebral oxygen levels following global cerebral ischemia–reperfusion injury without improving CI or brain tissue perfusion. After resuscitation, a complex series of events occur during reperfusion, which leads to secondary brain damage¹⁰. The beneficial effects of levosimendan have been the subject of numerous studies¹¹ that have reported increased ROSC rates^{3,12} and reduced rates of post-resuscitation myocardial dysfunction¹³, brain injury⁴, and kidney ischemia/reperfusion injury¹⁴. The combination of hypothermia and levosimendan has a positive effect on cardiac function, and survival has been shown to improve following CA in the rat¹⁵. Such positive effects have been attributed to enhanced cardiac output¹¹ or CBF⁴ as the underlying mechanism. However, in contrast to this assumption, we found that levosimendan did not improve CI, any of the hemodynamic parameters, or cortical perfusion. Our

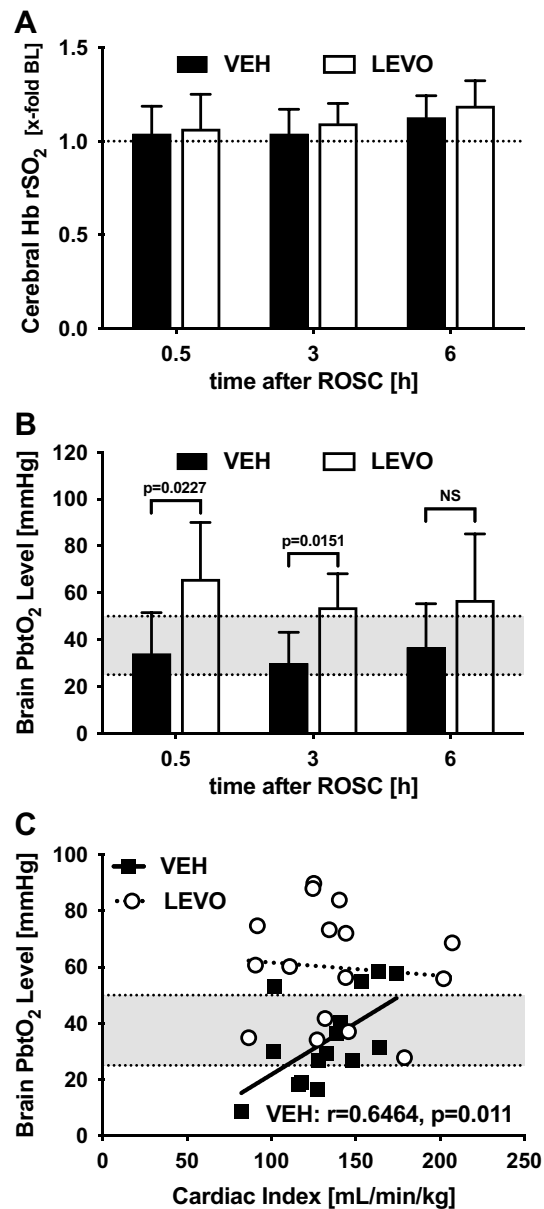


Figure 4. Cerebral tissue oxygenation. (A) Brain oxygenation was determined noninvasively by quantifying brain hemoglobin (Hb) oxygen saturation (rSO₂) before and 0.5, 3, and 6 h after ROSC. Because of high interindividual differences, readings were normalized to baseline. rSO₂ was not altered following cardiac arrest and did not differ between groups. *VEH* vehicle; *LEVO* levosimendan. Statistics: repeated measures two-way ANOVA, followed by Šidák's multiple comparisons test; data are presented as means ± SD. (B) Brain tissue oxygen (PbtO₂) was measured using a Foxy probe 14 mm below the dura in the left hemisphere 0.5, 3, and 6 h after ROSC. Levosimendan-treated animals showed significantly higher PbtO₂ 30 min and 3 h after ROSC. The normal PbtO₂ range (25–50 mmHg) is illustrated by the gray area. Statistics: Welch's t test; data are presented as means ± SD. (C) Correlation analysis between PbtO₂ and cardiac index (CI) showed a significant association between cardiac function and PbtO₂ in vehicle-treated animals, whereas levosimendan-treated animals had normal PbtO₂ and showed no correlation between PbtO₂ and CI. The normal PbtO₂ range (25–50 mmHg) is illustrated by the gray area. Statistics: Spearman rank correlation coefficient.

study confirms findings from a study in healthy pigs without signs of left ventricular dysfunction, which showed that levosimendan does not enhance cardiac function¹⁶.

There is a growing body of evidence for a neuroprotective mechanism of levosimendan that is independent of any cardio-circulatory effect. Following transient spinal ischemia, levosimendan has been shown to ameliorate neurological damage⁸ and reperfusion injury in a middle cerebral artery occlusion rat model¹⁷, without affecting systemic hemodynamic parameters. Moreover, in an in vitro model of traumatic brain injury, levosimendan reduces secondary tissue injury⁷.

We showed that levosimendan improves PbtO_2 30 min after CA, without influencing perfusion at the microcirculatory or macrocirculatory level. This uncoupling between CBF and tissue oxygenation is highly relevant because cerebral oxygenation is considered to be directly dependent on cerebral flow. Interestingly, tissue oxygenation in the buccal mucosa has also shown to be improved by levosimendan compared with norepinephrine in a rat model of septic shock, without major changes in microcirculation or general hemodynamics¹⁸. We are confident that our dataset is highly reliable because precise methods were used to measure tissue oxygenation¹⁹ and tissue perfusion, such as the gold standard fluorescence microspheres method, O₂C, and NIRS²⁰.

In summary, cardiac output, cerebral perfusion, and tissue oxygenation data suggested that levosimendan acts at the cellular level by improving mitochondrial function. The present results may offer the missing link between *in vitro* and *in vivo* studies. A putative mechanism of action is the activation of $\text{mitoK}_{\text{ATP}}$ ²¹. Levosimendan has also been shown to interact with hydrophobic targets of respiratory chain complexes by lowering the function of the respiratory chain and possibly reducing ischemia/reperfusion injury in subsarcolemmal mitochondria²².

The selected methods required tissue digestion to liberate microbeads to accurately quantify perfusion. Thus, it was not possible to perform molecular or histological analyses of brain tissue. Further investigations are required to confirm the role of $\text{mitoK}_{\text{ATP}}$ and the respiratory chain complex in the observed influence of levosimendan on brain tissue oxygenation. Additionally, healthy animals that do not show cardiovascular comorbidities that are typically observed in patients with CA of cardiac origin were used in this study. Hence, the present study largely represents the clinical situation of CA due to hypoxia or hypovolemia.

Conclusion

Optimal cerebral oxygenation is key to minimizing neurological damage during and following CA. We showed that NIRS does not reliably detect low PbtO_2 levels and that levosimendan improves parenchymal brain oxygen content. This effect was not accompanied by an increase in cardiac output or cerebral perfusion. Thus, our data suggest a direct levosimendan-mediated effect at the cellular level, which suggests that levosimendan presents a promising therapeutic approach for rescuing brain tissue in patients with acute and critically low tissue oxygen levels following CA, stroke, or traumatic brain injury.

Methods

Subjects. The study was approved by the Federal Animal Ethics Committee (Landesuntersuchungsamt Rheinland-Pfalz, Koblenz; protocol number 23 177-07/G 13-1-0103) and performed in accordance with the ARRIVE guidelines and general local and federal regulations and guidelines. We made every effort to minimize the number of animals used and their suffering. A total of 19 male pigs (body weight: 28.4 ± 3.1 kg; age: 2 months) were subjected to CA and resuscitation and were then randomized to receive levosimendan or vehicle treatment. Three animals did not achieve ROSC after the second defibrillation and were therefore excluded before randomization. All other animals showed ROSC after the second defibrillation.

Cardiac arrest (CA). To minimize stress during transportation from the animal facility to the laboratory all animals were sedated with an intramuscular injection of ketamine (8 mg/kg) and midazolam (0.2 mg/kg). Anesthesia was induced by intravenous injections of fentanyl (4 $\mu\text{g}/\text{kg}$) and propofol (3 mg/kg) and was maintained by continuous infusion of fentanyl (8 $\mu\text{g}/\text{kg}/\text{h}$) and propofol (8 mg/kg/h). A single dose of atracurium (1.5 mg/kg) was administered before endotracheal intubation. Volume-controlled ventilation (AVEA Care-Fusion, San Diego, CA) was conducted (tidal volume, 8 mL/kg; positive end-expiratory pressure 5 cmH_2O , $\text{FiO}_2 = 0.3$; inspiration-to-expiration ratio, 1:2; and variable respiration rate to achieve an end-tidal, $\text{pCO}_2 < 6$ kPa). Temperature was monitored continuously using a rectal probe and maintained with a heating blanket.

Using ultrasound for guidance, five femoral vascular catheters were placed: one triple-lumen central venous catheter in the right femoral vein, a 5F introducer sheath in the right femoral artery for an arterial pressure catheter placed in the thoracic descending aorta, one introducer sheath in the left femoral vein for a pacing catheter, two introducer sheaths in the left femoral artery for a PiCCO cardiac output system (Pulsion Medical Systems, Feldkirchen, Germany) and a LV-catheter for a microsphere injection placed in the left cardiac ventricle. The position of the LV-catheter was verified via pressure curve and pressure values unique to the position in the left ventricle.

Following baseline measurements, CA was induced with a pacing catheter in the right cardiac ventricle. After ventricular fibrillation (VF), ventilation and general anesthesia were discontinued. Immediately following 7 min of VF, ventilation was started at a rate of 10 min^{-1} , external chest compressions were initiated with a thumping device (LUCAS 2[®], Physio-Control Inc., Lund, Sweden) at a rate of 100 min^{-1} , and 0.4 U/kg of vasopressin was injected. After 2 min of persisting VF, an initial defibrillation at 200 J was performed and an additional 0.4 U/kg of vasopressin was administered. Subsequently, chest compressions were continued for 2 min, followed by a second defibrillation at 360 J. All animals included in the study achieved ROSC after the second defibrillation. ROSC was defined as a presence of heart contractions and mean arterial blood pressure (MAP) above 30 mmHg. Immediately after ROSC, 30 mL/kg of balanced electrolyte solution (Sterofundin iso, B. Braun, Melsungen, Germany) were given, anesthesia was resumed, and the animals received either 12 $\mu\text{g}/\text{kg}$ of levosimendan (LEVO), followed by continuous infusion of 0.3 $\mu\text{g}/\text{kg}/\text{min}$ or the equivalent fluid volume of balanced electrolyte solution (BES). Randomization and preparation of the infusion were carried out by a third party who was not involved in the experimental setting.

Following ROSC, norepinephrine infusion was started in all animals at a rate of 0.3 $\mu\text{g}/\text{kg}/\text{min}$. If MAP was below 60 mmHg at 5 min after ROSC, an additional balanced electrolyte solution bolus (15 mL/kg) was administered. Target MAP was defined as 75 ± 10 mmHg. Further norepinephrine infusion was adjusted accordingly.

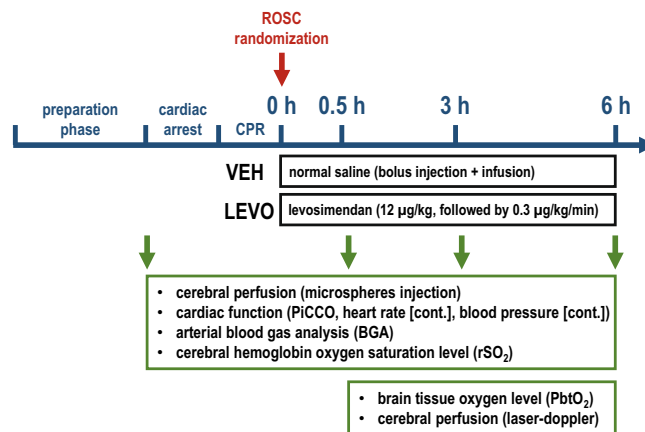


Figure 5. Experimental protocol.

Balanced electrolyte solution infusion was adjusted to 5 mL/kg/h, and additional boluses were injected if the global end-diastolic volume index (GEDV) dropped below 20% of the baseline value (before CPR).

Investigators were blind to the experimental groups. Apart from the continuous infusion of levosimendan or vehicle solution, both groups were treated identically (see Fig. 5).

Hemodynamic variables and blood gas analysis. An arterial thermo-dilution system (PiCCO System) was used to determine and record blood pressure, cardiac index (CI), GEDV, intrathoracic blood volume index (ITBI), and systemic vascular resistance index (SVRI). All parameters were measured and recorded continuously (S5, GE Healthcare, USA). Arterial blood gas analysis was performed with a Rapidlab 248 system (Bayer Healthcare, Germany).

Brain hemoglobin oxygen saturation. We quantified cerebral oxygen hemoglobin saturation (rSO₂) using a near-infrared spectroscopy (NIRS) probe (Adult Soma Sensor, Covidien, Mansfield, MA, USA) placed on the right forehead. Measured values were updated and displayed in 5 s intervals using the INVOS™ 5100C cerebral/somatic oximeter (Somanetics Corporation, Troy, MI, USA).

Cerebral tissue oxygen. PbtO₂ content was measured using an ultrafast fiber-optic, aluminum-jacketed fluorescence-quenching pO₂ probe with an uncoated ruthenium complex at the tip (Foxy-AL300, Ocean Optics, Dunedin, FL)¹⁹.

A craniotomy (1 × 1 cm) was performed on the left hemisphere, 5 mm apart from the midline and 5 mm behind the coronal suture, to allow insertion of the probe (diameter 0.5 mm) through and 14 mm below the dura.

Laser Doppler flowmetry. Cerebral microcirculation was measured using the laser Doppler flowmetry (O2C) system (LEA Medizintechnik, Gießen, Germany). Based on the Doppler principle and light spectroscopy, the system measures regional blood flow 8 mm below the surface. The probe was positioned 1 cm lateral to the Foxy-AL300 probe on the intact dura.

Cerebral perfusion by microspheres. The colored microsphere technique was used to measure regional blood flow as previously described^{23,24}. In brief, fluorescent-labeled microspheres (15 µm diameter) were injected via a catheter into the left cardiac ventricle to be distributed throughout the body and trapped in capillaries. Four different colors were used in a randomized sequence at baseline (BL, before CPR) and 30 min, 3 h, and 6 h after ROSC (1 mL equaling 10⁶ spheres). At the end of the observation period animals were euthanized, brains and kidneys removed and separated into small samples to facilitate recovery of the microspheres by digesting the samples. The number of microspheres were determined via high-performance liquid chromatography for a highly sensitive quantification of the fluorescence levels. They were injected via a catheter into the left ventricle to be distributed throughout the body and trapped in capillaries. Four different colors were used in a randomized sequence. At baseline (BL, before CPR) and 30 min, 3 h, and 6 h after ROSC, 1 mL (equaling 10⁶ spheres) was injected. After the animals were euthanized, the complete brain and kidneys were dissected, and the microspheres were recovered.

Statistical analysis. All experiments were performed after randomization, and the experiments and analyses were performed by investigators who were all blind to group allocation. The Prism 9 statistical software (GraphPad, La Jolla, CA, USA) was used to perform statistical analysis. Before the analysis, we assessed the test assumptions. Because of the limited power of small samples, we did not perform formal goodness-of-fit tests before the t test or analysis of variance (ANOVA); instead, we relied on the graphical assessment of distribution characteristics. Normality was determined by inspecting the unimodality and symmetry of histograms as well as by Q–Q plots. The equality of variances was determined by inspecting the histograms and standard deviations

(SDs). To evaluate group differences in repeated measurements from the same animals, a repeated measures two-way ANOVA was applied (factors: treatment and time), which was followed by a Šidák multiple comparisons test. Comparisons between two independent groups were conducted using Welch's *t* test. A *p* value of < 0.05 was considered statistically significant. Correlation analysis between PbtO₂ and CI was performed using the Spearman rank correlation coefficient. Data are presented as means and SDs (means ± SD).

Ethics approval and consent to participate. Experiments were approved by the Federal Animal Care Committee (Landesuntersuchungsamt Rheinland-Pfalz, protocol number 23 177-07/G 13-1-0103). The experiments were performed in accordance with the ARRIVE guidelines and general local and federal regulations and guidelines.

Consent for publication. The manuscript does not include details, images, or videos relating to an individual person.

Data availability

All datasets generated and analyzed during this study are kept in the Dept of Anesthesiology, Medical Center of the Johannes Gutenberg-University and are available from the corresponding author upon reasonable request.

Received: 18 May 2021; Accepted: 28 June 2021

Published online: 09 July 2021

References

- Ashana, D. C. *et al.* Determining the association between end-of-life care resources and patient outcomes in Pennsylvania ICUs. *Crit. Care Med.* <https://doi.org/10.1097/CCM.0000000000003969> (2019).
- Berger, R. *et al.* Levosimendan and prostaglandin E1 for uptitration of beta-blockade in patients with refractory, advanced chronic heart failure. *Eur. J. Heart Fail.* **9**, 202–208. <https://doi.org/10.1016/j.ejheart.2006.06.001> (2007).
- Koudouna, E. *et al.* Levosimendan improves the initial outcome of cardiopulmonary resuscitation in a swine model of cardiac arrest. *Acta Anaesthesiol. Scand.* **51**, 1123–1129. <https://doi.org/10.1111/j.1399-6576.2007.01383.x> (2007).
- Kelm, R. F. *et al.* Effects of levosimendan on hemodynamics, local cerebral blood flow, neuronal injury, and neuroinflammation after asphyctic cardiac arrest in rats. *Crit. Care Med.* **42**, e410–419. <https://doi.org/10.1097/CCM.0000000000000308> (2014).
- Onody, P. *et al.* Levosimendan: A cardiovascular drug to prevent liver ischemia-reperfusion injury?. *PLoS ONE* **8**, e73758. <https://doi.org/10.1371/journal.pone.0073758> (2013).
- Papp, Z. *et al.* Levosimendan: Molecular mechanisms and clinical implications: Consensus of experts on the mechanisms of action of levosimendan. *Int. J. Cardiol.* **159**, 82–87. <https://doi.org/10.1016/j.ijcard.2011.07.022> (2012).
- Roehl, A. B. *et al.* Neuroprotective properties of levosimendan in an in vitro model of traumatic brain injury. *BMC Neurol.* **10**, 97. <https://doi.org/10.1186/1471-2377-10-97> (2010).
- Lafci, B. *et al.* Protection of the spinal cord from ischemia: Comparative effects of levosimendan and iloprost. *Eur. Surg. Res.* **41**, 1–7. <https://doi.org/10.1159/000121394> (2008).
- Klein, K. U. *et al.* Transmission of arterial oxygen partial pressure oscillations to the cerebral microcirculation in a porcine model of acute lung injury caused by cyclic recruitment and derecruitment. *Br. J. Anaesth.* **110**, 266–273. <https://doi.org/10.1093/bja/aes376> (2013).
- Nolan, J. P. *et al.* Post-cardiac arrest syndrome: Epidemiology, pathophysiology, treatment, and prognostication: A scientific statement from the International Liaison Committee on Resuscitation; the American Heart Association Emergency Cardiovascular Care Committee; the Council on Cardiovascular Surgery and Anesthesia; the Council on Cardiopulmonary, Perioperative, and Critical Care; the Council on Clinical Cardiology; the Council on Stroke (Part 1). *Int. Emerg. Nurs.* **17**, 203–225. <https://doi.org/10.1016/j.ienj.2009.01.001> (2009).
- Varvarousi, G., Stefaniotou, A., Varvaroussis, D., Aroni, F. & Xanthos, T. The role of Levosimendan in cardiopulmonary resuscitation. *Eur. J. Pharmacol.* **740**, 596–602. <https://doi.org/10.1016/j.ejphar.2014.06.024> (2014).
- Wu, B. *et al.* Supplement of levosimendan to epinephrine improves initial resuscitation outcomes from asphyxial cardiac arrest. *BMC Anesthesiol.* **17**, 18. <https://doi.org/10.1186/s12871-017-0309-3> (2017).
- Huang, L., Weil, M. H., Tang, W., Sun, S. & Wang, J. Comparison between dobutamine and levosimendan for management of postresuscitation myocardial dysfunction. *Crit. Care Med.* **33**, 487–491 (2005).
- Grossini, E. *et al.* Levosimendan protection against kidney ischemia/reperfusion injuries in anesthetized pigs. *J. Pharmacol. Exp. Ther.* **342**, 376–388. <https://doi.org/10.1124/jpet.112.193961> (2012).
- Wang, C. H., Chang, W. T., Tsai, M. S., Huang, C. H. & Chen, W. J. Synergistic effects of moderate therapeutic hypothermia and levosimendan on cardiac function and survival after asphyxia-induced cardiac arrest in rats. *J. Am. Heart Assoc.* **9**, e016139. <https://doi.org/10.1161/JAHA.120.016139> (2020).
- Oldner, A. *et al.* Effects of levosimendan, a novel inotropic calcium-sensitizing drug, in experimental septic shock. *Crit. Care Med.* **29**, 2185–2193 (2001).
- Hein, M. *et al.* Levosimendan limits reperfusion injury in a rat middle cerebral artery occlusion (MCAO) model. *BMC Neurol.* **13**, 106. <https://doi.org/10.1186/1471-2377-13-106> (2013).
- Fries, M. *et al.* Levosimendan but not norepinephrine improves microvascular oxygenation during experimental septic shock. *Crit. Care Med.* **36**, 1886–1891. <https://doi.org/10.1097/CCM.0b013e31817ced9> (2008).
- Klein, K. U. *et al.* A novel technique for monitoring of fast variations in brain oxygen tension using an uncoated fluorescence quenching probe (Foxy AL-300). *J. Neurosurg. Anesthesiol.* **23**, 341–346. <https://doi.org/10.1097/ANA.0b013e31822cf893> (2011).
- Klein, K. U. *et al.* Intraoperative monitoring of cerebral microcirculation and oxygenation—A feasibility study using a novel photo-spectrometric laser-Doppler flowmetry. *J. Neurosurg. Anesthesiol.* **22**, 38–45. <https://doi.org/10.1097/ANA.0b013e3181bea439> (2010).
- Kopustinskiene, D. M., Pollesello, P. & Saris, N. E. Levosimendan is a mitochondrial K(ATP) channel opener. *Eur. J. Pharmacol.* **428**, 311–314 (2001).
- Sommer, S. *et al.* Impact of levosimendan and ischaemia-reperfusion injury on myocardial subsarcolemmal mitochondrial respiratory chain, mitochondrial membrane potential, Ca²⁺ cycling and ATP synthesis. *Eur. J. Cardiothorac. Surg.* **49**, e54–62; discussion e62. <https://doi.org/10.1093/ejcts/ezv397> (2016).
- Rudolph, A. M. & Heymann, M. A. The circulation of the fetus in utero. Methods for studying distribution of blood flow, cardiac output and organ blood flow. *Circ. Res.* **21**, 163–184 (1967).

24. Morsbach, S. *et al.* Quantification of fluorescent dyes in organ tissue samples via HPLC analysis. *J. Chromatogr. B Anal. Technol. Biomed. Life Sci.* **1072**, 34–39. <https://doi.org/10.1016/j.jchromb.2017.11.012> (2018).

Acknowledgements

We thank D. Dirvonskis and B. Müller for their excellent technical assistance. Some of the data presented in this article are part of the doctoral thesis of NK presented to the Johannes Gutenberg-University Mainz.

Author contributions

A.G.B., S.C.T., R.F.K., and E.K.H. designed the studies. A.G.B., J.K., A.Z., T.L., and N.K. conducted the experiment and data collection. B.D., S.M., K.M., A.H., and N.K. processed and analyzed tissue for microspheres measurements. A.G.B. and S.C.T. analyzed the data and wrote the manuscript. S.C.T. and E.K.H. reviewed the manuscript and finally approved it for publication.

Funding

Open Access funding enabled and organized by Projekt DEAL. This work was supported by a grant from the Johannes Gutenberg-University Mainz (Stage 1 grant, RFK).

Competing interests

The authors declare no competing interests.

Additional information

Correspondence and requests for materials should be addressed to A.G.-B. or S.C.T.

Reprints and permissions information is available at www.nature.com/reprints.

Publisher's note Springer Nature remains neutral with regard to jurisdictional claims in published maps and institutional affiliations.



Open Access This article is licensed under a Creative Commons Attribution 4.0 International License, which permits use, sharing, adaptation, distribution and reproduction in any medium or format, as long as you give appropriate credit to the original author(s) and the source, provide a link to the Creative Commons licence, and indicate if changes were made. The images or other third party material in this article are included in the article's Creative Commons licence, unless indicated otherwise in a credit line to the material. If material is not included in the article's Creative Commons licence and your intended use is not permitted by statutory regulation or exceeds the permitted use, you will need to obtain permission directly from the copyright holder. To view a copy of this licence, visit <http://creativecommons.org/licenses/by/4.0/>.

© The Author(s) 2021